



## ISTITUTO NAZIONALE DI RICERCA METROLOGICA Repository Istituzionale

Density Measurements of Two Liquefied Biomethane-Like Mixtures over the Temperature Range from (100 to 180) K at Pressures up to 9.0 MPa

*Original*

Density Measurements of Two Liquefied Biomethane-Like Mixtures over the Temperature Range from (100 to 180) K at Pressures up to 9.0 MPa / Cavuoto, Giuseppe; von Preetzmann, Nils; Eckmann, Philipp; Li, Jianrong; van der Veen, Adriaan M. H.; Kleinrahm, Reiner; Richter, Markus. - In: INTERNATIONAL JOURNAL OF THERMOPHYSICS. - ISSN 0195-928X. - 42:3(2021). [10.1007/s10765-020-02791-9]

*Availability:*

This version is available at: 11696/80401 since: 2024-03-05T10:16:24Z

*Publisher:*

Springer

*Published*

DOI:10.1007/s10765-020-02791-9

*Terms of use:*

This article is made available under terms and conditions as specified in the corresponding bibliographic description in the repository

*Publisher copyright*

SPRINGER NATURE OPEN ACCESS

This article is licensed under a Creative Commons Attribution 4.0 International License, which permits use, sharing, adaptation, distribution and reproduction in any medium or format, as long as you give appropriate credit to the original author(s) and the source, provide a link to the Creative Commons licence, and indicate if changes were made. The images or other third party material in this article are

(Article begins on next page)



# Density Measurements of Two Liquefied Biomethane-Like Mixtures over the Temperature Range from (100 to 180) K at Pressures up to 9.0 MPa

Giuseppe Cavuoto<sup>1</sup> · Nils von Preetzmann<sup>2</sup> · Philipp Eckmann<sup>3</sup> ·  
Jianrong Li<sup>4</sup> · Adriaan M. H. van der Veen<sup>4</sup> · Reiner Kleinrahm<sup>2</sup> ·  
Markus Richter<sup>3</sup>

Received: 18 December 2020 / Accepted: 31 December 2020 / Published online: 3 February 2021  
© The Author(s) 2021

## Abstract

Densities of two synthetic biomethane-like mixtures were measured in the homogeneous liquid phase and the supercritical region using a low-temperature single-sinker magnetic-suspension densimeter. Both mixtures consist of methane, nitrogen, hydrogen and oxygen, whereas the second mixture additionally contains carbon dioxide. For the first mixture, four isotherms from (100 to 160) K were studied over the pressure range from (1.5 to 6.6) MPa. The second mixture was investigated along three isotherms from (140 to 180) K at pressures of (2.6 to 9.0) MPa, where only the densities at 180 K are usable due to solidification of the carbon dioxide at the lower temperatures. The relative expanded combined uncertainty ( $k=2$ ) of the experimental densities was estimated to be in the range of (0.022 to 0.027) % for the first mixture and (0.046 to 0.054) % for the second mixture, respectively. Due to a supercritical liquefaction procedure and the integration of a special VLE-cell, densities in the homogeneous liquid phase could be measured without changing the composition of the liquefied mixture. Moreover, saturated-liquid densities were determined by extrapolation of the experimental single-phase liquid densities to the vapor pressure, which was determined experimentally for the mixture without carbon dioxide and calculated with an equation of state (EOS) for the mixture containing carbon dioxide. The relative expanded combined uncertainty ( $k=2$ ) of the saturated-liquid densities is less than 0.08 % in most cases. The new experimental results were compared with the GERG-2008 equation of state; the deviations are less than 0.17 %.

**Keywords** Cryogenic state · Density measurement · Liquefied biomethane mixtures · Magnetic-suspension coupling · Single-sinker densimeter

---

✉ Markus Richter  
m.richter@mb.tu-chemnitz.de

Extended author information available on the last page of the article

## 1 Introduction

Liquefied biomethane (LBM), also known as liquefied biogas (LBG), bio liquefied natural gas (bio-LNG) or renewable LNG, is a climate-neutral fuel with a comparatively large energy density. LBM essentially combines the benefits of LNG and carbon neutrality. In a recent study, Gustafsson and Svensson report that using LNG as a transport fuel involves less greenhouse gas emissions only under certain circumstances, while “there are clear environmental incentives to use LBM” [1]. However, for LBM, it currently seems problematic “to compete economically with the price of LNG, due to the higher specific production costs”. Nevertheless, in the future, there appears to be a realistic chance that LBG gets competitively viable as the supply chain is evidently simpler than the conventional one for LNG [2, 3]. Since the utilization of LNG and LBG as transport fuel is part of the European Union clean fuel strategy, the Joint Research Project “Metrological support for LNG and LBG as transport fuel” was funded as part of the European Metrology Programme for Innovation and Research (EMPIR) with the overall aim to enable the large-scale roll-out of LNG and LBG as a transport fuel. This includes to achieve smaller uncertainties in the determination of the LNG’s and LBG’s energy quantity during custody transfer, and here, one of the key properties is the density.

In our last paper [4], we presented density measurements of a (0.99 methane + 0.01 butane) mixture and a (0.98 methane + 0.02 isopentane) mixture over the temperature range from (100 to 160) K at pressures up to 10.8 MPa. This was done to test the performance of the EOS-LNG of Thol et al. [5], which is a new fundamental equation of state particularly developed for LNG mixtures that includes binary specific departure functions for butanes and pentanes; for this development, mainly the data of Lentner et al. [6] was used. Within the work of Eckmann et al. [4], we demonstrated that the EOS-LNG could improve the density prediction for LNG containing butane and isopentane compared to the GERG-2008 equation of state of Kunz and Wagner [7, 8], and we delivered accurate data for further improvement of the EOS-LNG.

Here, we report the results of accurate density measurements of two liquefied biomethane-like mixtures over the temperature range from (100 to 180) K at pressures up to 9.0 MPa, utilizing a special single-sinker densimeter for cryogenic liquid mixtures [4, 6, 9–12]. For both mixtures, the methane mole fraction is larger than 0.95, and the further components are nitrogen, hydrogen, and oxygen; one of the mixtures also contains carbon dioxide. Such measurements of biomethane-like mixtures, in particular in the homogeneous liquid phase and the supercritical region, at low temperatures and over a wide pressure range are unique so far. To the best of our knowledge, measurements like reported here have not been carried out elsewhere before as already discussed in our earlier papers [4, 6, 9–12]; other authors only measured data for saturated-liquid densities of binary mixtures and LNG-like mixtures [13–21] but not in the homogeneous liquid region below the cricondenbar pressure. For the two mixtures studied in the present work, however, no measurements of saturated-liquid densities could be found in literature.

Hence, the new  $(p, \rho, T, x)$  data that we measured can be used to test the performance of the GERG-2008 equation of state [7, 8] regarding these two methane-rich multicomponent mixtures with compositions typical for biomethane. (We note that the EOS-LNG was solely improved towards the methane + butanes and pentanes binaries, thus, there is no difference in the performance of EOS-LNG and the GERG-2008 equation of state for the mixtures investigated in this work.)

## 2 Experimental Section

### 2.1 Apparatus Description

A single-sinker magnetic-suspension densimeter, particularly developed for cryogenic liquid mixtures, was utilized; it covers a temperature range from (90 to 300) K at pressures up to 12 MPa. The densimeter's design, temperature and pressure measurement as well as the implementation of a special "VLE-cell" were described in detail previously [9–11]. A schematic diagram of the densimeter, presented by Richter et al. [11], is given in the Online Resource 1. In one of our latest papers [6], we presented a few improvements of the core apparatus to reduce diffusion effects and the force-transmission error (FTE) [22, 23]. Here, we summarize the description of the apparatus presented by Richter et al. [11]. Overviews of this general type of densimeter were provided by Wagner and Kleinrahm [24] as well as by McLinden [25].

The single-sinker method basically allows an absolute determination of the fluid density. This method is applied in conjunction with a magnetic-suspension coupling and a load compensation mechanism (differential method). A sinker of known volume  $V_S(T, p)$  and known mass  $m_S$  (in the present case: a single-crystal silicon,  $m_S \approx 60.95$  g,  $V_S \approx 26.17$  cm<sup>3</sup>,  $\rho_S \approx 2.329$  g · cm<sup>-3</sup>) is weighed while immersed in fluid of interest inside a pressure-tight measuring cell. Thus, the result of weighing the sinker located in the fluid,  $m_{S,fluid}^*$ , is the difference between the mass of the sinker and the buoyancy of the fluid:

$$m_{S,fluid}^* = m_S - \rho_{fluid} \cdot V_S(T, p), \quad (1)$$

where  $\rho_{fluid}$  denotes the fluid density. When weighing the sinker inside the evacuated measuring cell via the magnetic-suspension coupling, the weighing result is not the mass of the sinker,  $m_S$ , but a slightly different result,  $m_{S,vac}^*$ , which is the result of a small FTE of the magnetic-suspension coupling [22, 23]. Rearranging Eq. (1) yields the fluid density:

$$\rho_{fluid} = \frac{m_{S,vac}^* - m_{S,fluid}^*}{V_S(T, p)}. \quad (2)$$

Equation (2) actually requires additional terms since essential details of the measurement procedure (*e.g.*, the correction of the FTE) as discussed by Richter et al. (see reference [11], Appendix A) have to be taken in account. Moreover, the

problem of the FTE due to the magnetic-suspension coupling is described in detail by Kleinrahm et al. [23].

For the measurement of fluid density, the sinker is connected to an analytical balance (resolution: 0.01 mg) employing an appropriate coupling/decoupling device. Gravity and buoyancy forces acting on the sinker are transmitted to the balance via the magnetic-suspension coupling, thus, isolating the fluid sample (which may be at high pressure and very low temperature) from the balance, which is at ambient conditions. For compensation of the balance's zero-point drift, the weighing procedure considers the small drift of the balance reading in the tare position by subtracting it from the balance reading in the measuring position. The balance is operated near its tare point using a load compensation mechanism for reduction of possible errors of the balance due to changes in the slope of the characteristic curve over the weighing range.

## 2.2 Experimental Material

The two synthetic biomethane mixtures were gravimetrically prepared and delivered in steel cylinders with an internal volume of 50 dm<sup>3</sup> from a commercial supplier (Praxair Inc.). The desired compositions of the mixtures to be measured were previously specified by the collaborators within the EMPIR project. The gas mixtures have been produced from high-purity starting materials, to minimize effects from impurities on the density measurements. The mole fractions of the main components have been determined by comparison with the Dutch primary measurement standards in accordance with ISO 6143 [26] using gas chromatography with a thermal conductivity detector; a description of the instrument configuration and measurement procedure can be found elsewhere [27]. This procedure establishes the metrological traceability of the measured mole fractions as well as the smallest uncertainties, both required to obtain credible reference data. Results of the analyses, which are metrologically traceable to primary and internationally accepted measurement standards, are listed in Table 1. The stated uncertainties in composition were reported by the Dutch Van Swinden Laboratorium (VSL) in the calibration certificates as expanded uncertainties ( $k=2$ ), whereby the underlying standard uncertainties were determined according to the Guide to the expression of uncertainty in measurement (GUM) [28]. Further information on the mixtures is summarized in Tables 1 and 2. These are relevant for the experimental procedures described in Sect. 2.3.

To prevent any kind of change of the mixture composition (*e.g.*, due to phase separation), the sample was handled very carefully. Filling the sample into the measuring cell of the densimeter with the correct composition was essential. Hence, the sample cylinder was prepared according to the following procedure: (1) Rolling the sample cylinder for at least two hours to re-homogenize the gas mixture. (2) Heating the cylinder at the bottom part for at least 3 h using a heating jacket to obtain vortices inside the sample cylinder for homogenizing the gas. (3) Filling the gas mixture into the well-evacuated system to a pressure of about 0.2 MPa through the evacuated filling line and leaving the sample with a residence time of about two minutes before

**Table 1** Composition, standard uncertainties ( $k=1$ ) for each component, and molar mass  $M$  of the studied mixtures

Component	Mole fraction (certificate) <sup>a</sup>	Std. uncertainty ( $k=1$ ) [mole fraction (certificate) <sup>a</sup> ]	Mole fraction (normalized) <sup>b,c</sup>	Std. uncertainty ( $k=1$ ) [mole fraction (normalized) <sup>c</sup> ]
<i>LBG I</i>				
CH <sub>4</sub>	0.950800	0.000950	0.950053	0.000101
N <sub>2</sub>	0.035030	0.000090	0.035003	0.000093
H <sub>2</sub>	0.009960	0.000025	0.009952	0.000027
O <sub>2</sub>	0.004996	0.000013	0.004992	0.000014
$M/(\text{g}\cdot\text{mol}^{-1})$	–	–	16.4015	–
<i>LBG II</i>				
CH <sub>4</sub>	0.950400	0.000950	0.950128	0.000082
CO <sub>2</sub>	0.024960	0.000060	0.024953	0.000063
N <sub>2</sub>	0.009980	0.000025	0.009977	0.000027
H <sub>2</sub>	0.009980	0.000025	0.009977	0.000027
O <sub>2</sub>	0.004966	0.000013	0.004965	0.000013
$M/(\text{g}\cdot\text{mol}^{-1})$	–	–	16.7990	–

<sup>a</sup>As reported in the certificate of VSL. Uncertainties were determined in accordance with GUM [28]

<sup>b</sup>The calculation of physical and chemical properties of gas mixtures requires that the gas composition, expressed in mole fractions of all components in the mixture, adds up to 1. If the composition of the mixture is calculated from gravimetric preparation, then by default it adds up to 1 and is thereby ‘normalized’ [29, 30]. This procedure has been applied to the non-normalized data obtained from the comparison with the primary measurement standards

<sup>c</sup>The composition and uncertainty of the two gas mixtures have been normalized according to ISO 6974-2 [30]

**Table 2** Additional information on the studied mixtures relevant for the supercritical liquefaction procedure

Mixture	$p_{\text{Cyl}}/\text{MPa}^{\text{a}}$	$p_{\text{C}}/\text{MPa}^{\text{b}}$	$T_{\text{C}}/\text{K}^{\text{b}}$	$p_{\text{ccp}}/\text{MPa}^{\text{b}}$	$T_{\text{ccT}}/\text{K}^{\text{b}}$
LBG I	12.3	4.966	189.10	4.977	189.11
LBG II	12.0	5.044	192.88	5.050	192.92

<sup>a</sup>Initial pressure in the sample cylinder ( $V=50 \text{ dm}^3$ )

<sup>b</sup>The critical temperature  $T_{\text{C}}$ , the critical pressure  $p_{\text{C}}$ , the cricondenbar pressure  $p_{\text{ccp}}$  and the cricondentherm temperature  $T_{\text{ccT}}$  were calculated with the GERG-2008 equation of state [7, 8]

evacuating the apparatus again. Step (3) was repeated three times before the final filling. Thereby, residual gas from previously studied samples is removed to prevent an unwanted compositional change of the new sample filled into the densimeter.

### 2.3 Experimental Procedures

The details of filling the densimeter and the basic procedure of operating the apparatus are reported by Richter et al. [11]. We already used this procedure for our previous density measurements on synthetic LNG mixtures and methane-rich binary

mixtures [4, 6, 11, 12]. In the present work, this established procedure was applied for density measurements of two synthetic biomethane-like mixtures. Here, it is important to mention that our densimeter involves the application of a special VLE-cell, which serves as a buffer for the unavoidable phase transition (vapor–liquid) between the very cold measuring cell and the pressure measurement circuit that is kept at a constant temperature of about 313.15 K. The temperatures of the measuring cell and the VLE-cell can be controlled independently of each other at different set points. Since all areas of the measurement system are interconnected, the pressure is everywhere the same (apart from a pressure head correction).

At first, we filled the densimeter at ambient temperature to a pressure higher than the cricondenbar pressure (*e.g.*,  $p_{\text{fill}}=9.0$  MPa for present measurements); for example, see Fig. 1. Then, the measuring cell and the VLE-cell were cooled simultaneously at constant pressure by continuously adding sample to the system until the VLE-cell had reached a slightly subcritical temperature or at least a temperature considerably below the temperature at the cricondenbar pressure  $p_{\text{ccp}}$ . We maintained this temperature of the VLE-cell at a constant value, while the measuring cell was cooled further to the desired temperature and finally controlled to maintain a constant value. Thereby, the filling procedure was completed, and the first density value at  $p > p_{\text{ccp}}$  was measured. The composition determined for the gas mixture in the sample cylinder before filling the densimeter remained unchanged for the following density measurements in the homogeneous liquid phase.

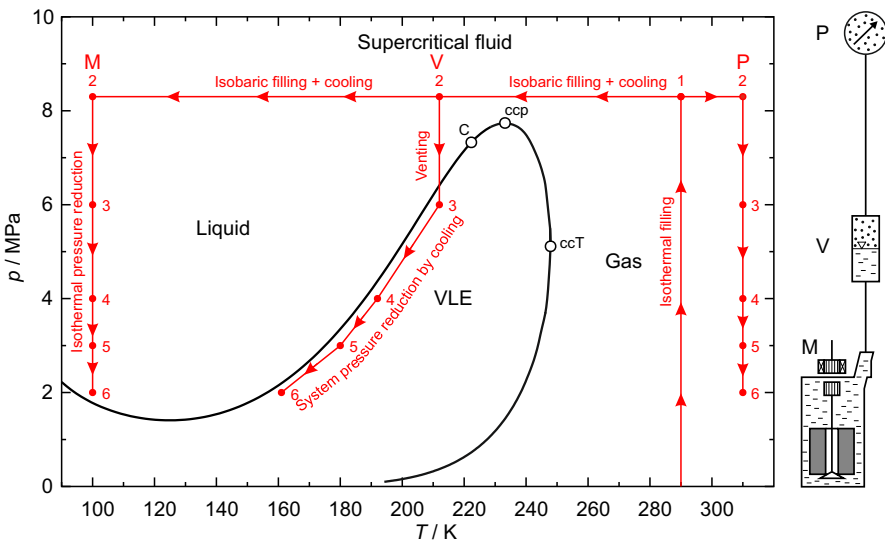


**Fig. 1** Left: Principle of the filling and liquefaction procedure shown in a  $p$ ,  $T$ -diagram for a methane-rich gas mixture containing hydrogen. As an example, the points to be measured at  $T=100$  K are plotted. For illustration purposes, a composition was chosen that differs from the mixtures investigated in this work (compare with Fig. S3 in the Online Resource 1). The phase envelope was calculated using the GERG-2008 equation of state of Kunz and Wagner [7, 8]. Right: Schematic presentation of the measurement system consisting of the measuring cell (M), VLE-cell (V) and pressure measurement system (P)

After the first density measurement above  $p_{\text{ccp}}$  (point 2 in Fig. 1), the pressure was reduced by venting gaseous sample from the system. This pressure reduction, at approximately constant temperature of the VLE-cell, results in a vapor–liquid equilibrium forming in the VLE-cell. The venting was stopped, when a liquid volume fraction of about 30 % was established in the VLE-cell (point 3 in Fig. 1). The respective pressure for the set-point temperature of the VLE-cell can be approximately calculated with the GERG-2008 equation of state [7, 8] in advance. At this point, the next density measurement was carried out.

To measure densities at further  $(p, T)$  state points in the homogeneous liquid phase, the pressure in the system was no longer adjusted by venting sample from the system but via reducing the temperature of the VLE-cell. Hence, from this point on, the total mass of fluid inside the system remained constant. By reducing the temperature of the VLE-cell, the pressure in the entire system was decreased accordingly to measure the points 4 to 6 (see Fig. 1). The last point 6 was always measured close to the calculated saturated-liquid line. The respective VLE-cell temperature for a desired pressure was determined via mass balance calculations using the GERG-2008 equation of state [7, 8]. The determined temperature was always just a little above the saturation temperature for the desired pressure and mixture composition, resulting in a liquid volume fraction in the VLE-cell between (30 and 70) %. For each investigated isotherm, we filled the densimeter separately.

## 2.4 Uncertainty in Density Measurement

The uncertainty in density measurement was determined in accordance with the GUM [28]. Assuming that there is no correlation between the input quantities, the expanded combined uncertainty  $U$  for the determination of cryogenic liquid densities using the above described densimeter can be calculated from:

$$U(\rho) = k \cdot u_c(\rho(T, p, \mathbf{x})) = k \cdot \left[ \begin{array}{c} u(\rho)^2 + \left( \left( \frac{\partial \rho}{\partial p} \right)_T \cdot u(p) \right)^2 + \left( \left( \frac{\partial \rho}{\partial T} \right)_p \cdot u(T) \right)^2 \\ + u(\rho(\mathbf{x}))^2 + u(\rho_{\text{repro}})^2 + u(\rho_{\text{corr}})^2 \end{array} \right]^{1/2}, \quad (3)$$

where  $u(\rho)$ ,  $u(T)$  and  $u(p)$  denote the standard uncertainties in density, temperature and pressure, respectively;  $u(\rho(\mathbf{x}))$  corresponds to the standard uncertainty in density resulting from the uncertainty of the gas composition;  $u(\rho_{\text{repro}})$  accounts for an additional uncertainty from the reproducibility of our measurements; and  $u(\rho_{\text{corr}})$  takes into account the uncertainty of the correction of the force-transmission error. A detailed description of the uncertainty evaluation has been reported in previous works [6, 11, 12]. The expanded combined uncertainty in measurement was estimated for each measured state point. Table 3 shows the contributions to the relative combined expanded uncertainty in density of an exemplary density measurement of the LBG I mixture at  $T=140$  K and  $p=3.02424$  MPa.

One of the main contributions (up to 68 % and 82 % for LBG I and LBG II, respectively) to the combined standard uncertainty in density originates from the



**Table 3** Uncertainty budget for the density measurements. As an example, the uncertainty was calculated for the LBG I mixture at  $T=140.000$  K,  $p=3.02424$  MPa, and  $\rho_{exp}=386.559$  kg·m<sup>-3</sup> (see Table 4)

Source of uncertainty	Expanded uncertainty <sup>a</sup> ( $k=2$ or 1.73)	Distribution	Standard uncertainty (%)
Density measurement	0.0080 %	Normal	0.0040
Pressure measurement	0.010 % · $p_{max}$ <sup>b</sup>	Rectangular	0.0004
Temperature measurement	15 mK	Rectangular	0.0043
Composition of the gas mixture	see Table 1 <sup>c</sup>	Normal	0.0078
Reproducibility of the measurements	0.0100 %	Normal	0.0050
Density correction <sup>d</sup>	0.0060 %	Normal	0.0030
Relative expanded combined uncertainty in density ( $k=2$ ): $U(\rho_{exp})=0.0227$ %			

<sup>a</sup>The expanded uncertainty of the individual sources is the same for both mixtures, except for the composition of a mixture (see Table 1)

<sup>b</sup>The value of  $p_{max}$  corresponds to the maximum pressure of the utilized pressure transmitter ( $p_{max}=13.8$  MPa, 3.45 MPa, and 0.69 MPa), which depends on the investigated pressure range

<sup>c</sup>For mixtures with more than two components, the uncertainty in density resulting from the gas analysis is a correlated uncertainty considering every individual component’s uncertainty. The contribution to the uncertainty in density is determined analogous to ISO 6976 [31]

<sup>d</sup>Correction of the measured densities due to the force-transmission error (FTE); see Sect. 3.7 in Richter et al. [11]. To correct the influence of the FTE, the (uncorrected) measured densities have been corrected between (+0.0026 and +0.0240) % for both oxygen-containing mixtures; see also Kleinrahm et al. [23], Appendixes A2 and A3. After correction of the FTE, its contribution on the density uncertainty ( $k=2$ ) is 0.0060 %

uncertainty in the gas composition  $u(\rho(x))$ . Here, it has to be considered that variations in composition of the individual components are correlated, which requires to consider the covariances between the mole fractions in the uncertainty evaluation. As described in ISO 6976 [31], the combined standard uncertainty in density due to the uncertainty in composition can be calculated by

$$u(\rho(x))^2 = \sum_{i=1}^N \sum_{j=1}^N \frac{\partial \rho}{\partial x_i} \cdot (x_i) \cdot r(x_i, x_j) \cdot u(x_j) \cdot \frac{\partial \rho}{\partial x_j}, \tag{4}$$

where  $N$  is the total number of components in the respective mixture (see Table 1) and  $\partial \rho / \partial x_i$  are the sensitivity coefficients for each respective component. The values for  $\partial \rho / \partial x_i$  were calculated with the GERG-2008 equation of state [7, 8] for each specific state point measured. The correlation coefficients  $r(x_i, x_j)$  for the components  $i$  and  $j$  were calculated according to ISO 14912 [32] by

$$r(x_i, x_j) = \frac{u(x_i, x_j)}{u(x_i) \cdot u(x_j)} \tag{5}$$

with

$$u(x_i, x_j) = -x_i u^2(x_j) - x_j u^2(x_i) + x_i x_j \sum_{k=1}^N u^2(x_k) / \left( \sum_{k=1}^N x_k \right)^2, \quad (6)$$

where  $u(x_i, x_j)$  is the covariance matrix and  $u(x_i)$  are the normalized uncertainties of the components in mole fraction (see Table 1).

### 3 Results and Discussion

The densities of two selected synthetic biomethane-like mixtures were measured in the homogeneous liquid phase and the supercritical region. Furthermore, saturated-liquid densities were determined.

#### 3.1 Results for Homogeneous Liquid and Supercritical Densities

For LBG I, the densities were measured along isotherms at  $T=(100, 120, 140$  and  $160)$  K and for LBG II at  $T=(140, 160$  and  $180)$  K; six state points were investigated along each isotherm. Starting always with the supercritical filling pressure and ending close to the saturated-liquid pressure, a pressure range from about (1.5 to 9.0) MPa was covered. To avoid a change in composition for the liquefied samples, the filling of the apparatus was carried out at pressures at least 0.5 MPa above the cricondenbar pressure  $p_{ccp}$  (see Table 2). Furthermore, to avoid vaporization of the mixture in the measuring cell, all measurements in the liquid phase were carried out at pressures at least 0.1 MPa above the saturation pressure  $p_{sat,GERG}$ , calculated with the GERG-2008 equation of state [7, 8]. Two or three replicates were measured at each  $(p, T)$  state point, and in total 24  $(p, \rho, T, x)$  data are reported for LBG I and 6 for LBG II.

The density measurements of the LBG II mixture at  $T=(140$  and  $160)$  K revealed that parts of the carbon dioxide contained in the mixture solidified. This assumption could be verified by a  $p, T$ -phase diagram of the LBG II mixture, which is attached in the Online Resource 1. The solidification resulted in a change in composition of the studied liquid, and the measured densities show large deviations from densities calculated with the GERG-2008 equation of state [7, 8], namely about  $-1.9\%$  at  $T=160$  K and  $-4.4\%$  at  $T=140$  K. Moreover, during these density measurements, the analytical balance readings showed a strong scatter of the values and a temporal drift. Based on the measured densities, we approximately estimated a change of the carbon dioxide mole fraction in the liquid phase from originally about  $2.5\%$  to about (1.6 and 0.3) % at  $T=(160$  and  $140)$  K, respectively. Hence, only the measurements along the isotherm at  $T=180$  K yielded reliable results.

The experimental results of the  $(p, \rho, T, x)$  measurements of the LBG I and the LBG II mixture are listed in Table 4 together with the corresponding state point uncertainties as discussed in Sect. 2.4. The relative expanded combined uncertainty ( $k=2$ ) in density was estimated to be equal to or less than  $0.027\%$  for LBG I and between (0.046 and 0.054) % for LBG II. The difference between these

**Table 4** Experimental densities<sup>a</sup> for two synthetic biomethane-like mixtures (compositions see Table 1) and relative deviations of experimental densities  $\rho_{\text{exp}}$  from densities  $\rho_{\text{GERG}}$  calculated with the GERG-2008 equation of state of Kunz and Wagner [7, 8] (as implemented in the TREND 4.0 software package [33]), where  $p$  is the pressure,  $T$  is the temperature (ITS-90), and  $100 (U(\rho)/\rho)$  is the relative expanded combined uncertainty ( $k=2$ ). The measurements were carried out in the homogenous liquid phase and the supercritical region

$p/\text{MPa}$	$\rho_{\text{exp}}/(\text{kg} \cdot \text{m}^{-3})$	$100 (U(\rho)/\rho)$	$100 (\rho_{\text{exp}} - \rho_{\text{GERG}})/\rho_{\text{GERG}}$
<i>LBG I</i>			
$T = 100.000 \text{ K}^b$			
6.45816	454.141	0.027	0.0085
4.51031	452.636	0.027	0.0080
3.52241	451.856	0.026	0.0077
2.53473	451.065	0.026	0.0074
1.99827	450.630	0.026	0.0073
1.50029	450.223	0.026	0.0071
$T = 120.000 \text{ K}^b$			
6.52363	425.227	0.025	0.0056
4.50902	423.000	0.025	0.0064
3.50016	421.846	0.025	0.0064
2.53369	420.715	0.025	0.0070
1.99778	420.076	0.025	0.0072
1.49864	419.473	0.025	0.0071
$T = 140.000 \text{ K}^b$			
6.52179	392.763	0.023	-0.0024
4.50791	389.298	0.023	-0.0034
3.81298	388.036	0.023	-0.0041
3.02424	386.559	0.023	-0.0048
2.50241	385.552	0.023	-0.0058
1.79965	384.158	0.022	-0.0069
$T = 160.000 \text{ K}^b$			
6.56414	354.000	0.021	-0.0302
4.50893	347.442	0.021	-0.0478
4.01343	345.678	0.021	-0.0534
3.51753	343.824	0.021	-0.0597
3.02510	341.882	0.022	-0.0668
2.72245	340.631	0.022	-0.0723
<i>LBG II</i>			
$T = 180.000 \text{ K}^b$			
9.02334	331.169	0.046	-0.0252
8.03268	326.495	0.046	-0.0347
7.00638	320.967	0.047	-0.0516
6.02140	314.747	0.049	-0.0750
5.03174	307.090	0.051	-0.1167
4.37683	300.759	0.054	-0.1627

<sup>a</sup>The expanded uncertainty ( $k=1.73$ ) in temperature is  $U(T)=0.015 \text{ K}$ . The expanded uncertainty ( $k=1.73$ ) in pressure is  $U(p)=0.01 \% \cdot p_{\text{max}}$ . The value of  $p_{\text{max}}$  corresponds to the maximum pressure of the three utilized pressure transmitters ( $p_{\text{max}}=0.69 \text{ MPa}$ ,  $3.45 \text{ MPa}$ , and  $13.8 \text{ MPa}$ ); we used the transmitters up to approximately  $0.8 \cdot p_{\text{max}}$ , i.e., ( $>0.18$  to  $\leq 0.50$ ;  $>0.50$  to  $\leq 2.7$ , and  $>2.7$

**Table 4** (continued)

to  $\leq 10.8$ ) MPa, respectively. According to our experience, the transmitters then show a better long-term stability of the calibration curve

<sup>b</sup>The measured temperatures were rounded to the even target temperatures. Accordingly, the experimental densities were corrected using the sensitivity of density to temperature  $(\delta\rho_{\text{EOS}}/\delta T)_p$  calculated with the GERG-2008 equation of state of Kunz and Wagner [7, 8]. For a maximum temperature correction of less than 100 mK, the uncertainty of density correction due to the uncertainty of the equation of state can be neglected in the uncertainty budget of the relative expanded combined experimental uncertainty ( $k=2$ ). A table with the uncorrected temperatures and densities is given in Online Resource 1

two uncertainties is mainly caused by the higher contribution of the uncertainty in composition of LBG II; *i.e.*, the consideration of five instead of four mixture components.

We would like to mention that a new equation of state for liquefied natural gases (LNG) was recently published by Thol et al. [5]; it is called EOS-LNG. This model is based on the GERG-2008 equation of state [7, 8] and enhances this equation with respect to the prediction of mixtures containing butanes and pentanes. Since these components were not contained in the mixtures investigated within this work, the GERG-2008 equation of state [7, 8] and the EOS-LNG [5] yield the same densities. Therefore, the GERG-2008 equation of state [7, 8] as an established model in the LNG community is used for the comparisons within this section.

The relative deviations of the experimental densities from values calculated with the GERG-2008 equation of state [4, 5] (as implemented in the TREND 4.0 software package [33]) are also reported in Table 4. In Fig. 2, the relative deviations of the experimental densities from values calculated with the GERG-2008 equation

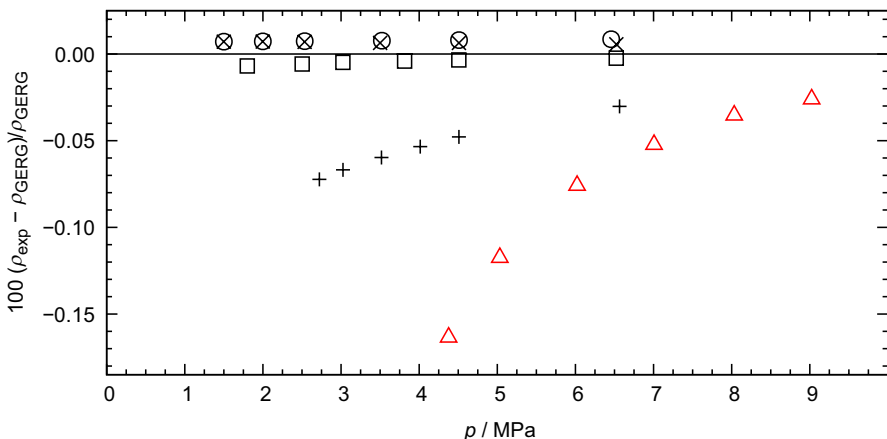


**Fig. 2** Relative deviations of experimental densities  $\rho_{\text{exp}}$  for from densities  $\rho_{\text{GERG}}$  calculated with the GERG-2008 equation of state [7, 8] (zero line).  $(p, \rho, T, x)$  data measured in the present work. LBG I:  $\circ$ ,  $T=100$  K;  $\times$ ,  $T=120$  K;  $\square$ ,  $T=140$  K;  $+$ ,  $T=160$  K. LBG II:  $\triangle$ ,  $T=180$  K. The compositions of the LBG mixtures are given in Table 1

of state are plotted versus pressure. The relative deviations for the LBG I mixture are less than  $\pm 0.01\%$  for  $T=(100, 120$  and  $140)$  K but increase up to  $-0.072\%$  at  $T=160$  K. The experimental densities of the LBG II mixture at  $T=180$  K deviate by up to  $-0.1627\%$  from values calculated with the GERG-2008 equation of state, with increasing deviations towards lower pressures.

The authors of the GERG-2008 report uncertainties for binary systems only [7, 8]. Based on these uncertainties, we estimated an uncertainty of the GERG-2008 equation of state of  $0.3\%$  for the calculated densities of the LBG I and II mixtures in the liquid phase. Hence, the GERG-2008 equation of state describes the experimental data clearly within this uncertainty.

### 3.2 Determination of Saturated-Liquid Densities

For both LBG mixtures, saturated-liquid densities in the temperature range from (100 to 180) K were determined by extrapolation of the experimental densities in the homogenous liquid region to the mixture's vapor pressure. The results are listed in Table 5. The influence of the extrapolation on the uncertainty of the saturated-liquid densities is relatively small in most cases, except for the higher temperatures  $T \geq 160$  K.

The relative deviations of the experimental saturated-liquid densities of the two LBG mixtures from values calculated with the GERG-2008 equation of state [7, 8] are plotted in Fig. 3. The numerical values of these relative deviations are

**Table 5** Saturated-liquid densities<sup>a</sup>  $\rho_{\text{sat,exp}}$  for the two synthetic biomethane-like mixtures (compositions see Table 1) and their relative deviations from densities  $\rho_{\text{sat,GERG}}$  calculated with the GERG-2008 equation of state of Kunz and Wagner [7, 8] (as implemented in the TREND 4.0 software package [33]), where  $p_{\text{sat}}$  is the vapor pressure<sup>a</sup>,  $T$  is the temperature (ITS-90), and  $100(U(\rho)/\rho)$  is the relative expanded combined uncertainty ( $k=2$ )

$T/\text{K}$	$p_{\text{sat}}/\text{MPa}$	$\rho_{\text{sat,exp}}/(\text{kg} \cdot \text{m}^{-3})$	$100(U(\rho)/\rho)$	$100(\rho_{\text{sat,exp}} - \rho_{\text{sat,GERG}})/\rho_{\text{sat,GERG}}$
<i>LBG I</i>				
100.000	0.905	449.733	0.028	-0.0487
120.000	1.032	418.902	0.031	-0.0421
140.000	1.475	383.498	0.039	-0.0609
160.000	2.498	339.678	0.079	-0.0598
<i>LBG II</i>				
180.000	3.763	294.024	0.596	0.0455

<sup>a</sup>The saturated-liquid densities were determined by extrapolating the experimental densities along isotherms in the homogenous liquid region to the vapor pressure. The vapor pressure  $p_{\text{sat}}$  for the LBG II mixture was calculated from the GERG-2008 equation of state [7, 8]. Its relative expanded uncertainty ( $k=2$ ) was estimated by us to be  $3\%$  based on ref. [7]. For the LBG I mixture, the vapor pressures  $p_{\text{sat,exp}}$  were experimentally determined and their expanded absolute uncertainty ( $k=2$ ) was estimated to be  $0.06$  MPa (see Table 6). For  $T \geq 160$  K, the larger uncertainties of the extrapolated values,  $\rho_{\text{sat,exp}}$ , are caused by the larger isothermal compressibility  $(\partial\rho/\partial p)_T$  near the phase boundary in combination with the uncertainty of the calculated vapor pressure

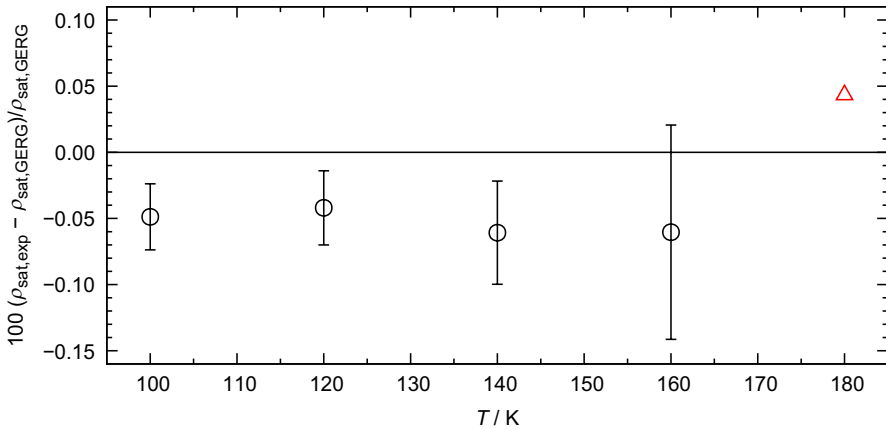


**Fig. 3** Relative deviations of experimental saturated-liquid densities  $\rho_{\text{sat,exp}}$  for two biomethane-like mixtures from densities  $\rho_{\text{sat,GERG}}$  calculated with the GERG-2008 equation of state [7, 8] (zero line). ( $\rho_{\text{sat}}$ ,  $\rho_{\text{sat}}$ ,  $T$ ,  $x$ ) data of the present work: LBG I:  $\circ$ ; BG II:  $\triangle$ . The uncertainties of our new saturated-liquid density data are illustrated with error bars (also see Table 5). For the LBG II mixture, no error bars are plotted since they are outside the scaling of the ordinate. The compositions of the LBG mixtures are given in Table 1

listed in Table 5. The uncertainty of the saturated-liquid densities of the two LBG mixtures calculated with the GERG-2008 equation of state was estimated by us to be 0.3 % (see Sect. 3.1). Hence, the GERG-2008 equation of state describes the new experimental saturated-liquid densities clearly within this uncertainty.

For the determination of the saturated-liquid densities, a cubic equation was fitted to the six experimental densities on each isotherm in the homogenous liquid phase. Then, these equations were extrapolated to the mixture’s vapor pressure. The vapor pressures needed for this extrapolation were usually calculated with the GERG-2008 equation of state [7, 8]. For the LBG II mixture at  $T = 180$  K it was  $p_{\text{sat}} = 3.763$  MPa; its relative expanded uncertainty ( $k = 2$ ) was estimated by us to be 3 %, based on ref. [7]. For the LBG I mixture, however, the saturated-liquid

**Table 6** Experimentally determined saturated-liquid pressures  $p_{\text{sat,exp}}$  for LBG I (composition see Table 1) and their absolute deviations from saturated-liquid pressures  $p_{\text{sat,GERG}}$  calculated with the GERG-2008 equation of state of Kunz and Wagner [7, 8], where  $U(p_{\text{sat,exp}})$  is the absolute expanded uncertainty ( $k = 2$ ) of the experimentally determined saturated-liquid pressures

$T/K$	$p_{\text{sat,exp}}/\text{MPa}$	$p_{\text{sat,GERG}}^a/\text{MPa}$	$U(p_{\text{sat,exp}})/\text{MPa}$	$(p_{\text{sat,exp}} - p_{\text{sat,GERG}})/\text{MPa}$
100.000	0.905	1.2086	0.06	-0.3036
120.000	1.032	1.1998	0.06	-0.1678
140.000	1.475	1.5760	0.06	-0.1010
160.000	2.498	2.4857	0.06	-0.0123

pressures calculated with the GERG-2008 equation of state for  $T < 160$  K are obviously incorrect. In this region, the saturated-liquid line in a  $\rho$ ,  $T$ -diagram shows a curvature from lower to higher pressures; see Fig. 4. This curvature is also depicted in a  $p$ ,  $T$ -diagram in Fig. S4 in the Online Resource 1. The reason for this unusual behavior is presumably the component hydrogen in the LBG mixture.

Therefore, we determined the saturated-liquid pressures of LBG I ourselves with our densimeter. The measurement procedure is explained in the Online Resource 1. The results are listed in Table 6. Since our densimeter is not suitable for the measurement of saturated-liquid pressures of fluid mixtures, the uncertainty of the results is relatively large; see Table 6. Moreover, saturation pressures calculated with the GERG-2008 equation of state [7, 8] and the difference of the experimental pressures from the calculated pressures are also given in the table.

The new  $(p, \rho, T, x)$  data measured in the homogeneous liquid region are depicted in a  $p$ ,  $T$ -diagram in Fig. 4. Furthermore, the saturated-liquid densities, which were determined by extrapolation of the six experimental densities on each isotherm in the homogeneous liquid region to the vapor pressure, are also shown.

It should be mentioned here that the GERG-2008 equation of state [7, 8] also yielded reasonable values for saturated-liquid densities  $\rho_{\text{sat,GERG}}(T)$ , even though the respective saturated-liquid pressures are higher than the experimentally determined values (see Fig. 4 and Table 6). Therefore, such calculated values were

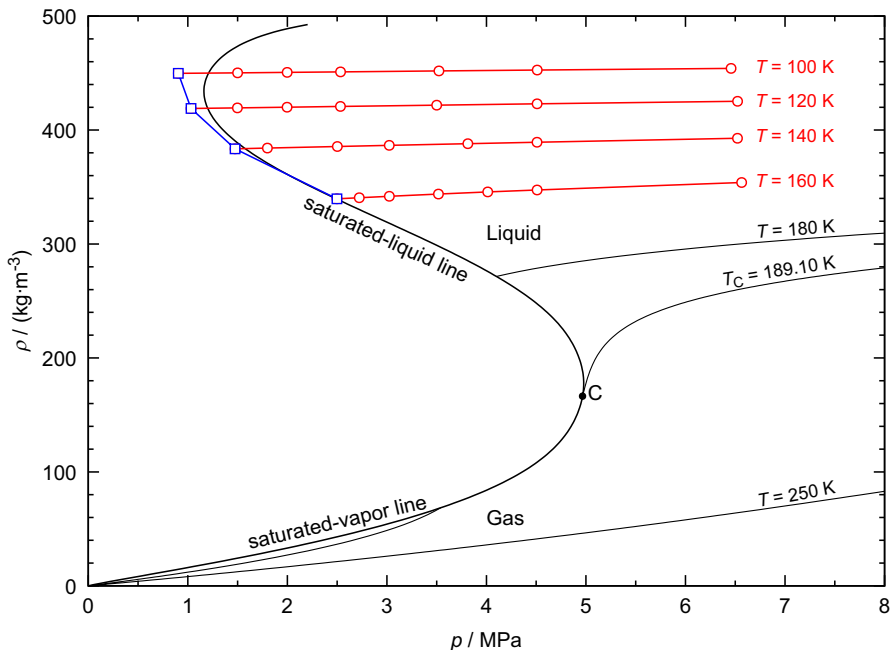


**Fig. 4**  $\rho$ ,  $p$ -diagram of LBG I (see Table 1 for composition). The phase boundary and the isotherms were calculated with the GERG-2008 equation of state of Kunz and Wagner [7, 8];  $\circ$ ,  $(p, \rho, T, x)$  state points measured in the present work;  $\square$ , saturated-liquid densities determined by extrapolation to the experimentally determined saturated-liquid pressure;  $\bullet$ , critical point

used in Table 5 and Fig. 3 for comparison with the new experimental saturated-liquid densities.

## 4 Conclusion

Accurate density measurements of two biomethane-like mixtures, LBG I and LBG II, were carried out along isotherms from  $T=(100$  to  $180)$  K at pressures up to 9.0 MPa, utilizing a special single-sinker densimeter for cryogenic liquid mixtures. Both mixtures consist of more than 95 mol-% methane and the three further components nitrogen, hydrogen, and oxygen; the LBG II mixture additionally contains carbon dioxide. The densities of the LBG I mixture were measured at  $T=(100, 120, 140,$  and  $160)$  K at six state points on each isotherm between the vapor pressure and  $p=6.6$  MPa. The LBG II mixture could only be measured at  $T=180$  K at six state points between the vapor pressure and  $p=9.0$  MPa. The reason was presumably the solidification of about (88 and 36) % of carbon dioxide at  $T=(140$  and  $160)$  K, respectively, of the original content of about 2.5 mol % in this mixture. A problem arose when determining the saturated-liquid densities of the LBG I mixture. These values were determined by extrapolation of the six density state points on each isotherm in the homogeneous liquid region to the mixture's vapor pressure. Since the vapor pressures calculated with the GERG-2008 equation of state [7, 8] were obviously incorrect for  $T\leq 160$  K, we measured the vapor pressures by ourselves with our densimeter.

The experimental results were compared with the GERG-2008 equation of state of Kunz and Wagner [7, 8]. The relative deviations of the new experimental values from densities calculated with the GERG-2008 equation of state are less than  $\pm 0.01$  % in the homogeneous liquid region of the LBG I mixture at  $T=(100, 120$  and  $140)$  K, and less than 0.08 % at  $T=160$  K. For the LBG II mixture, the relative deviations in the homogeneous liquid region are between  $-(0.02$  and  $0.17)$  % at  $T=180$  K. Thus, the GERG-2008 equation of state is able to describe the new experimental densities of both LBG mixtures within the uncertainty of 0.3 %, where this uncertainty was estimated by us based on the reported uncertainty by the authors of the GERG-2008 equation of state [7, 8] for binary mixtures.

**Supplementary Information** The online version contains supplementary material available at <https://doi.org/10.1007/s10765-020-02791-9>.

**Acknowledgements** We thank Professor Roland Span and Dr. Monika Thol of Ruhr University Bochum for helpful discussions regarding the present topic. Moreover, we are thankful to Santiago Castaños Benito for supporting the present project within the scope of his master thesis. This work was part of the Joint Research Project “Metrological support for LNG custody transfer and transport fuel applications” (Grant No. JRP: 16ENG09 LNG III) and was carried out as part of the European Metrology Programme for Innovation and Research (EMPIR), which was co-funded by the European Union's Horizon 2020 research and innovation programme and the EMPIR participating countries within the European Association of National Metrology Institutes (EURAMET).

**Funding** Open Access funding enabled and organized by Projekt DEAL.







**Open Access** This article is licensed under a Creative Commons Attribution 4.0 International License, which permits use, sharing, adaptation, distribution and reproduction in any medium or format, as long as you give appropriate credit to the original author(s) and the source, provide a link to the Creative Commons licence, and indicate if changes were made. The images or other third party material in this article are included in the article's Creative Commons licence, unless indicated otherwise in a credit line to the material. If material is not included in the article's Creative Commons licence and your intended use is not permitted by statutory regulation or exceeds the permitted use, you will need to obtain permission directly from the copyright holder. To view a copy of this licence, visit <http://creativecommons.org/licenses/by/4.0/>.

## References

1. M. Gustafsson, N. Svensson, J. Clean. Prod. (2021). <https://doi.org/10.1016/j.jclepro.2020.123535>
2. M.A. Qyyum, K. Qadeer, M. Lee, Ind. Eng. Chem. Res. (2018). <https://doi.org/10.1021/acs.iecr.7b03630>
3. M.A. Qyyum, J. Haider, K. Qadeer, V. Valentina, A. Khan, M. Yasin, M. Aslam, G. de Guido, L.A. Pellegrini, M. Lee, Renew. Sustain. Energy Rev. (2020). <https://doi.org/10.1016/j.rser.2019.109561>
4. P. Eckmann, N. von Preetzmann, G. Cavuoto, R. Kleinrahm, M. Richter, Int. J. Thermophys. (2020). <https://doi.org/10.1007/s10765-020-02728-2>
5. M. Thol, M. Richter, E.F. May, E.W. Lemmon, R. Span, J. Phys. Chem. Ref. Data (2019). <https://doi.org/10.1063/1.5093800>
6. R. Lentner, P. Eckmann, R. Kleinrahm, R. Span, M. Richter, J. Chem. Thermodyn. (2020). <https://doi.org/10.1016/j.jct.2019.106002>
7. O. Kunz, W. Wagner, J. Chem. Eng. Data (2012). <https://doi.org/10.1021/je300655b>
8. International Organization for Standardization, *ISO 20765-2:2015, Natural gas — Calculation of Thermodynamic Properties* (2015)
9. M. Richter, R. Kleinrahm, R. Span, P. Schley, A new apparatus for the accurate measurement of LNG densities. *GWF Int.* **1**, 66–69 (2010)
10. M. Richter, R. Kleinrahm, R. Span, P. Schley, *A new apparatus for accurate measurements of the densities of liquefied natural gas (LNG)*, Int. Gas. Res. Conf. Proc. pp. 2776–2790 (2011)
11. M. Richter, R. Kleinrahm, R. Lentner, R. Span, J. Chem. Thermodyn. (2016). <https://doi.org/10.1016/j.jct.2015.09.034>
12. R. Lentner, M. Richter, R. Kleinrahm, R. Span, J. Chem. Thermodyn. (2017). <https://doi.org/10.1016/j.jct.2017.04.002>
13. J. Klosek, C. McKinley, *Densities of liquefied natural gas and of low molecular weight hydrocarbons*. First International Conference on LNG, Chicago, 1968
14. J.B. Rodosevich, R.C. Miller, *AIChE J.* (1973). <https://doi.org/10.1002/aic.690190408>
15. M.J. Hiza, W.M. Haynes, W.R. Parrish, J. Chem. Thermodyn. (1977). [https://doi.org/10.1016/0021-9614\(77\)90173-2](https://doi.org/10.1016/0021-9614(77)90173-2)
16. R.C. Miller, M.J. Hiza, *Fluid Phase Equilib.* (1978). [https://doi.org/10.1016/0378-3812\(78\)80004-1](https://doi.org/10.1016/0378-3812(78)80004-1)
17. M. Hiza, W. Haynes, J. Chem. Thermodyn. (1980). [https://doi.org/10.1016/0021-9614\(80\)90109-3](https://doi.org/10.1016/0021-9614(80)90109-3)
18. W. Haynes, J. Chem. Thermodyn. (1982). [https://doi.org/10.1016/0021-9614\(82\)90077-5](https://doi.org/10.1016/0021-9614(82)90077-5)
19. W. Haynes, J. Chem. Thermodyn. (1983). [https://doi.org/10.1016/0021-9614\(83\)90123-4](https://doi.org/10.1016/0021-9614(83)90123-4)
20. J.E. Orrit, *Fluid Phase Equilib.* (1983). [https://doi.org/10.1016/0378-3812\(83\)80065-X](https://doi.org/10.1016/0378-3812(83)80065-X)
21. J. Janisch, G. Raabe, J. Köhler, J. Chem. Eng. Data (2007). <https://doi.org/10.1021/je700210n>
22. M.O. McLinden, R. Kleinrahm, W. Wagner, Int. J. Thermophys. (2007). <https://doi.org/10.1007/s10765-007-0176-0>
23. R. Kleinrahm, X. Yang, M.O. McLinden, M. Richter, Adsorption (2019). <https://doi.org/10.1007/s10450-019-00071-z>
24. W. Wagner, R. Kleinrahm, *Metrologia* (2004). <https://doi.org/10.1088/0026-1394/41/2/S03>
25. M.O. McLinden, in *Volume Properties*. ed. by E. Wilhelm, T. Letcher (Royal Society of Chemistry, Cambridge, 2014), p. 73
26. International Organization for Standardization, *ISO 6143:2001, Gas analysis — Comparison methods for determining and checking the composition of calibration gas mixtures* (2001)
27. A.M.H. van der Veen, E.T. Zalewska, D.R. van Osselen, T.E. Fernández, C. Gómez, J. Beránek, R.J. Oudwater, D.C. Sobrinho, M.C. Brum, C.R. Augusto, J. Fükö, T. Büki, Z. Nagyné Szilágyi, P.J. Brewer, M.L. Downey, R.C. Brown, M. Valkova, Z. Durisova, K. Arrhenius, B. Magnusson, H. Yaghooby, T.

- Tarhan, E. Engin, L.A. Konopelko, T.A. Popova, M.N. Pir, O.V. Efremova, *Metrologia* (2020). <https://doi.org/10.1088/0026-1394/57/1A/08011>
28. International Organization for Standardization, *JCGM 100:2008 — Evaluation of measurement data* (2008)
  29. International Organization for Standardization, *ISO 6974-1:2012, Natural gas — determination of composition and associated uncertainty by gas chromatography* (2012)
  30. International Organization for Standardization, *ISO 6974-2:2012, Natural gas — Determination of composition and associated uncertainty by gas chromatography* (2012)
  31. International Organization for Standardization, *ISO 6976:2016, Natural gas — Calculation of calorific values, density, relative density and Wobbe indices from composition* (2016)
  32. International Organization for Standardization, *ISO 14912:2003, Gas analysis — Conversion of gas mixture composition data* (2003)
  33. R. Span, R. Beckmüller, T. Eckermann, S. Herrig, S. Hielscher, A. Jäger, E. Mickoleit, T. Neumann, S. Pohl, B. Semrau, M. Thol, *TREND* (Prof. Dr.-Ing. Roland Span, Lehrstuhl für Thermodynamik, Ruhr-Universität Bochum (2019)

## Authors and Affiliations

Giuseppe Cavuoto<sup>1</sup> · Nils von Preetzmann<sup>2</sup>  · Philipp Eckmann<sup>3</sup> ·  
Jianrong Li<sup>4</sup>  · Adriaan M. H. van der Veen<sup>4</sup>  · Reiner Kleinrahm<sup>2</sup> ·  
Markus Richter<sup>3</sup> 

<sup>1</sup> Istituto Nazionale Di Ricerca Metrologica (INRiM), Torino, Italy

<sup>2</sup> Faculty of Mechanical Engineering, Thermodynamics, Ruhr University, Bochum, Germany

<sup>3</sup> Department of Mechanical Engineering, Applied Thermodynamics, Chemnitz University of Technology, Chemnitz, Germany

<sup>4</sup> Unit of Chemistry, Mass, Pressure, Viscosity, Van Swinden Laboratorium, Thijsseweg 11, Delft 2629 JA, The Netherlands